Positron trapping in an electrostatic well by inelastic collisions with nitrogen molecules

T. J. Murphy* and C. M. Surko
Physics Department, University of California, San Diego, La Jolla, California 92093
(Received 29 April 1992)

Positrons from a radioactive source are slowed to electron-volt energies and accumulated and stored in a trap which uses a magnetic field for radial confinement and an electrostatic well for axial confinement. The positrons lose energy and become trapped through inelastic collisions with nitrogen molecules introduced into the trap for this purpose. The trap has three stages with progressively lower nitrogen pressure. It is found that the trapping in each stage is due primarily to electronic excitation of the nitrogen molecules, with the energy loss being approximately 9 eV per collision. Positronium formation is believed to be the dominant loss mechanism during the trapping process. Trapping efficiencies of greater than 25% have been achieved. Using a 150-mCi ^{22}Na source, a maximum stored number of $\sim 1\times 10^7$ positrons have been stored with a lifetime of 40 s, limited by the annihilation on the nitrogen gas at a pressure of 2×10^{-6} Torr. The positrons cool to room temperature in a few seconds via rotational and momentum transfer collisions with the nitrogen.

PACS number(s): 34.90.+q, 34.50.Gb, 52.55.Mg, 52.20.Hv

I. INTRODUCTION

Positrons are the most common form of antimatter on the earth, but until recently they have only been studied as single particles after creation in the radioactive decay of certain isotopes or in pair production from high-energy electrons or photons. Their interactions with ordinary matter have been studied only as single positrons with atoms, molecules, or bulk matter.

Recent progress in the development of methods for trapping and storing positrons [1–5] has allowed the accumulation of sufficient low-temperature positrons that they form a pure positron plasma. This is, we believe, the first collective state of antimatter achieved in a laboratory.

The accumulation of large numbers of low-energy positrons allows the possibility of studying such unique systems as electron-positron plasmas [6]. In addition, the availability of a pulsed, intense source of positrons allows the possibility of a pulsed positronium beam for fusion plasma research [7–9]. The availability of large numbers of cold positrons also allows the study of positron-molecule and positron-atom interactions below the threshold for positronium formation, including the study of molecules which exist as solids or liquids at room temperature and atmospheric pressure, but which are gases at the pressures inside the trap [2,10–13].

In this paper, we describe the trapping and accumulation of positrons in a cylindrical trap in which confinement is provided by a potential well, and radial confinement by a magnetic field. In order for positrons to become trapped within the potential well, they must lose kinetic energy. Possible energy-loss mechanisms include inelastic collisions with atoms or molecules, radiation (such as bremsstrahlung or cyclotron radiation), and interactions with image currents in the trap walls. For the trapping scheme discussed in this paper, the energy-loss mechanism is the inelastic collision of positrons with a molecular species (specifically, nitrogen).

Positrons may lose energy to nitrogen molecules in several ways: ionization, electronic excitation, dissociation, vibrational excitation, rotational excitation, and momentum transfer. These processes occur at different rates depending on the energy of the collision, and all but the momentum-transfer mechanism have a threshold. In addition to these processes, positronium formation or direct annihilation may occur, leading to the loss of positrons from the system.

In the work described here, it is shown that the dominant mechanism for energy loss is the electronic excitation of nitrogen molecules. In the optimum case, this results in an average energy loss of approximately 9 eV per collision. This energy loss competes with positronium formation, which causes the loss of positrons from the system. It turns out that trapping is negligible for positrons with less than 8 eV. Above 11 eV, positronium formation is as efficient in causing the loss of positrons as electronic excitation is in trapping them. Thus, a "trapping gap" exists within which efficient trapping of positrons can occur.

This paper is organized as follows. Section II gives a detailed description of the apparatus used for studying the interactions of interest, and for trapping positrons. Section III describes the evolution of the energy distribution of the positrons as they pass through the nitrogen gas, experiencing collisions and losing energy. Section IV describes the trapping of positrons in an electrostatic well as a function of positron energy. Section V describes the use of a multistage electrostatic trap, with regions of progressively lower nitrogen pressure, for efficient trapping, accumulation, and long-term storage of positrons. This trap has been used in experiments to study the interaction of thermal positrons with atoms and molecules.

II. EXPERIMENTAL APPARATUS

The experimental apparatus used in this work consists of a radioactive source of positrons, a single-crystal

tungsten transmission moderator, and a multistage positron trap, with associated magnetic-field coils and vacuum systems.

For most of the experiments described here, the source of positrons was a 45-mCi ^{22}Na radioactive source ($\tau_{1/2}$=2.6 yr). This isotope emits positrons in 90% of the disintegrations with a continuous distribution of energies up to 545 keV. The positrons impinge upon a 1-μm single-crystal tungsten foil, where a certain fraction of them are stopped and thermalize. They then diffuse in the foil and some of the positrons reach the surface and are ejected nearly perpendicularly to the surface with an energy of about 2 eV. Efficiencies of up to 10^{-3} have been reported for this process [14–16]. For the experiments reported here, we estimate our moderator efficiency to be $(3\pm1)\times10^{-4}$ based on a total efficiency (ratio of the number of positrons entering the trap to the number of positrons formed in the source) of 5.4×10^{-5}. The uncertainty in moderator efficiency (ratio of moderated positrons in forward direction to positrons striking moderator) is due to uncertainty in the effective solid angle of the moderator and effects of scattering and self-absorption in the source. The moderator can be biased to produce monoenergetic positrons of any desired energy, and is generally operated at approximately 40 V, resulting in 42-eV positrons. The kinetic energy of the positrons is due almost entirely to the velocity of the positrons perpendicular to the moderator. The velocity distribution parallel to the moderator surface is Gaussian, with a width corresponding to an effective temperature between 0.4 and 0.6 eV. The magnetic field at the source and moderator is about 100 G. The positrons are magnetically guided from the moderator to the trapping region.

The trap is formed by a set of eight cylindrically symmetric electrodes (numbered 0 through 7) of varying length and radius [Fig. 1(a)]. These electrodes form regions of decreasing electric potential, and they are constructed to allow three-stage differential pumping of the system [Fig. 1(b)]. Pumping is provided by three 8-in. cryopumps: one is located at each end of the trap, and one is located in the middle of the trap which pumps through slots cut in the large diameter section of electrode 3. Nitrogen gas is introduced through a small hole in the middle of electrode 1. This pumping arrangement leads to three distinct regions of gas pressure. The high-pressure region (stage I) is formed by electrode 1 and has a typical pressure of 10^{-3} Torr. The middle region (stage II) is formed by electrodes 2 and 3, and has a typical pressure of 10^{-4} Torr. The final region (stage III) forms the trapping region where the positrons are accumulated, and is typically operated at 2×10^{-6} Torr. The electrode geometry of the final stage is based on the highly successful experiments to confine pure-electron plasmas [17]. It differs from the typical operation of a Penning trap in that the trapping region extends well beyond the central region where the potential is approximately hyperbolic, but extends to near the ends of the electrode where the potential increases quickly. In addition, the self-field of the positrons causes the expansion of the positron cloud along the magnetic axis away from the center where confinement occurs in the typical Penning geometry.

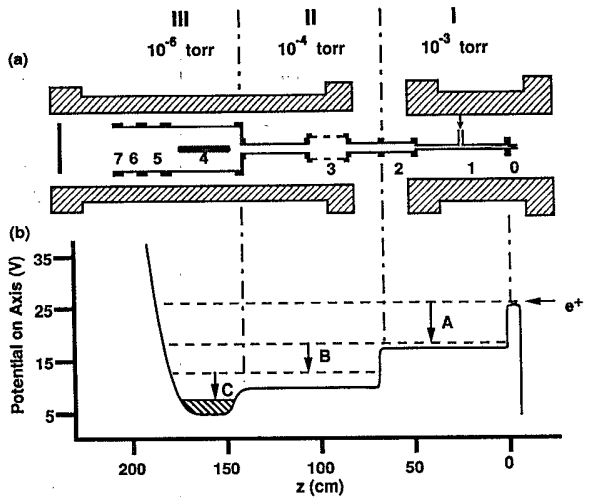

FIG. 1. (a) Electrode structure of the positron trap. Gas is injected in the center of electrode 1 (at the location of the arrow), and is pumped out through the ends and through the center of electrode 3, which has slots cut in it for that purpose. (b) Schematic representation of the trapping scheme, showing three stages of progressively lower electric potential and pressure. Positrons enter from the right and are ultimately trapped in the shaded portion of region III.

A magnetic field is applied along the axis of the trap using two solenoids. The first solenoid applies a field to electrodes 0, 1, and 2, and is capable of producing a field of up to 3000 G. The second solenoid applies a field to electrodes 3 through 7 and is capable of up to 1500 G. Typically, we operate at approximately 700 G.

Positrons enter the trap by passing over a potential barrier created by a voltage applied to electrode 0 [Fig. 1(b)]. The pressure is set so that, on average, the positron experiences one inelastic collision in traversing stage I [*A* in Fig. 1(b)]. The positron is then trapped within the electrode structure. It then experiences, in less than 1 ms, another collision (*B*) which traps it within regions II and III and finally, in a few tens of milliseconds, it experiences another collision (*C*) to trap it within region III. The positrons then cool to room temperature in a few seconds and are trapped in region III.

The trapped positrons are detected by lowering the voltage on the gate electrodes (typically electrodes 6 and 7), allowing the positrons to stream outwards along magnetic-field lines to be deposited on thin annihilation plates. A NaI(Tl) scintillator coupled to a photomultiplier tube is used to detect the radiation produced by the annihilation of the positrons in the plates. The annihilation plates are arranged in four concentric rings centered on the axis of the magnetic field. The plates may be biased independently to attract or repel positrons, allowing radial measurement of the positron density profile. In addition, charge-sensitive amplifiers have been used to measure the charge deposited on each of the rings directly.

III. SINGLE-PASS DISTRIBUTION

Positrons must become trapped within the electrode structure in a single pass through the system so that they do not reflect from the potential barrier formed by the gate electrode and return to the moderator where they would most likely annihilate. This first stage trapping sets an upper limit on the efficiency of trapping, and thus the physics of single-pass energy loss is extremely important.

The interaction of positrons with nitrogen in a single pass was studied by setting the potential of the first stage to 22 V, and using electrode 3 as an energy analyzing gate. The positrons are then detected by counting their annihilation rate on a plate at the far end of the trap as a function of this analyzing voltage. Only positrons with a parallel energy sufficient to overcome the retarding potential of this analyzer pass through the system. The others are either reflected or trapped in the first stage. For these measurements, the magnetic field was approximately 750 G in the first stage, and was approximately 430 G in the region of the analyzing electrode. This lower field near the analyzing electrode insured that magnetic mirroring did not lead to confinement in the first stage.

Figure 2 shows the derivative of the annihilation count rate with respect to analyzing potential as a function of analyzing potential for a number of different gas pressures in the first stage, which yields the parallel energy distribution after one pass. The broad distribution for the lowest gas pressure is due to the perpendicular energy of the positrons introduced at the moderator. This perpendicular energy increases as the positrons travel from the moderator region ($B \approx 100$ G) to the analyzer region ($B \approx 430$ G), due to the conservation of the magnetic moment $\mu \equiv E_\perp / B$.

As the pressure in the first stage is increased, the initial energy peak near 42 eV decreases, as a peak near 28 eV increases. This 28-eV peak then decreases as a peak near 24 eV increases. Since the energy distribution changes in this manner, rather than as a continuous decrease in energy, it appears that the energy loss occurs in well-defined steps. The location of the peaks can be explained as follows. The first peak, at the injected beam energy of 42 eV, is due to positrons which pass through the first stage without experiencing a single collision. If we assume that the positrons lose approximately 9 eV per collision, the resulting positron energy will be 33 eV. Since the potential of the first stage is 22 V, the positron has 11 eV of kinetic energy. If we further assume that the collisions produce an isotropic velocity distribution, then on average, two-thirds of this will be in the perpendicular (to the magnetic field) direction, and one-third in the parallel direction. However, in leaving the first stage and entering the analyzer region, the magnetic field decreases from 750 to 430 G. Thus, to conserve the magnetic moment, the perpendicular energy decreases to about 38% of the total kinetic energy in the first stage. Therefore, 62% of the kinetic energy that the positron has in the first stage is in the parallel component when the positron is in the analyzer region. This gives a total parallel energy of 28.8 eV, which agrees with the location of the second peak. A second collision, in which the positron again loses 9 eV, will leave the positron with 24 eV, of which 2 eV is kinetic energy in the first stage. An analysis along the lines of the above predicts a peak at 23.2 eV, also in good agreement with the observed third peak.

One can plot the area under each peak as a function of pressure in the first stage, and one obtains Fig. 3. For the first peak (no collisions), the area falls exponentially with increasing pressure. The second peak (one collision) first increases with pressure, and then decreases exponentially.

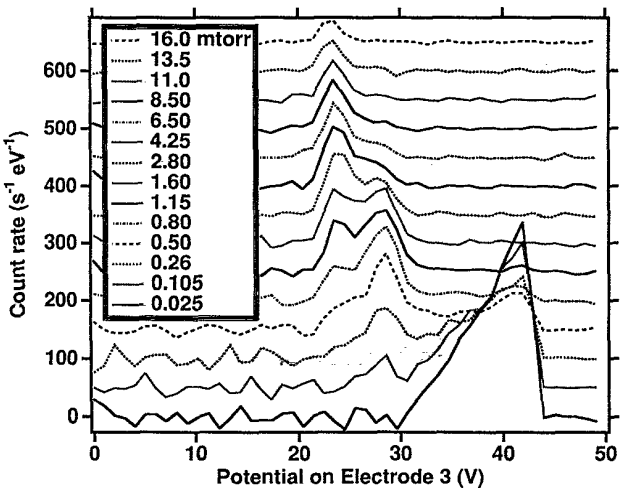

FIG. 2. Differential single-pass count rate for positrons passing through the trap showing the parallel energy distribution. *The curves* are offset vertically for clarity. The potential on the first stage was 22 V and positrons were injected with energy of 42 eV.

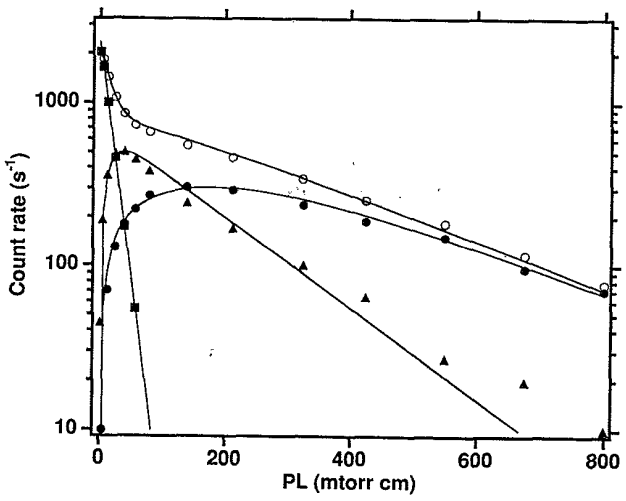

FIG. 3. Number of positrons in the three peaks identified in Fig. 2 as a function of the product of the pressure (P) and the path length (L) for the first state: (■) no collisions, (▲) one collision, (●) two collisions, and (○) the total number of positrons in all of the peaks. The solid lines represent the fit [Eq. (2)] using the parameters given in Table I.

The third peak (two collisions) increases slowly, followed by an exponential decrease. One may note that the transfer from the first peak to the second is not 100% efficient. This can be interpreted as being due to the formation of positronium by collisions with nitrogen. The positronium formation threshold in nitrogen is 8.8 eV, well below the 20-eV kinetic energy which the positrons have upon entering the first stage.

We have developed a model to explain the time behavior of the three peaks. We assume that the full-energy positrons can (1) form positronium and be lost, (2) experience a collision with an energy loss which results in a kinetic energy in the second peak, or (3) experience a collision with an energy loss which results in a kinetic energy in the third peak. We further assume that there is loss from the second and third peaks (i.e., from diffusion to the walls), as well as collisions in which positrons with energies in the second peak lose energy, resulting in energies in the third peak. These assumptions result in a set of coupled differential equations similar to those describing radioactive decay:

$$\begin{aligned}\frac{dN_1}{d\chi}&=-N_1(\lambda_{12}+\lambda_{13}+\lambda_{\mathrm{Ps}})\ ,\\ \frac{dN_2}{d\chi}&=N_1\lambda_{12}-N_2(\lambda_{23}+\lambda_{\mathrm{out2}})\ ,\\ \frac{dN_3}{d\chi}&=N_1\lambda_{13}+N_2\lambda_{23}-N_3\lambda_{\mathrm{out3}}\ ,\end{aligned}\tag{1}$$

where χ is the pressure-pathlength product, N_m is the number of positrons in peak m, λ_{mn} is the rate for moving directly from peak m to peak n, and $\lambda_{\mathrm{out}n}$ is the loss rate from peak n. The solution to these equations is

$$\begin{aligned}N_1(\chi)&=N_1(0)\exp(-\lambda_1\chi)\ ,\\ N_2(\chi)&=N_1(0)\frac{\lambda_{12}}{\lambda_2-\lambda_1}[\exp(-\lambda_1\chi)-\exp(-\lambda_2\chi)]\ ,\\ N_3(\chi)&=N_1(0)\frac{\lambda_{13}}{\lambda_{\mathrm{out3}}-\lambda_1}[\exp(-\lambda_1\chi)-\exp(-\lambda_{\mathrm{out3}}\chi)]\\ &\quad+N_1(0)\frac{\lambda_{12}\lambda_{23}}{\lambda_2-\lambda_1}\left[\left[\frac{1}{\lambda_{\mathrm{out3}}-\lambda_2}-\frac{1}{\lambda_{\mathrm{out3}}-\lambda_1}\right]\exp(-\lambda_{\mathrm{out3}}\chi)-\frac{1}{\lambda_{\mathrm{out3}}-\lambda_2}\exp(-\lambda_2\chi)+\frac{1}{\lambda_{\mathrm{out3}}-\lambda_1}\exp(-\lambda_1\chi)\right]\ ,\end{aligned}\tag{2}$$

where $\lambda_1=\lambda_{12}+\lambda_{13}+\lambda_{\mathrm{Ps}}$ and $\lambda_2=\lambda_{23}+\lambda_{\mathrm{out2}}$. As shown in Fig. 3, this model provides an adequate description of the data using the parameters listed in Table I. The pressure in the first stage is known only approximately. Therefore, while the relative importance of the various processes can be derived accurately, the absolute value of the cross sections may be in error by as much as a factor of 3, which is the approximate uncertainty in the pressure of the first stage due to the difficulty in measuring the pressure in the 1.5-cm-diam, 50-cm-long tube without significantly disturbing the gas flow.

Of particular importance is the ratio of the rates for energy loss to the total loss from the first peak. For the above model, this factor is $(\lambda_{12}+\lambda_{13})/(\lambda_{12}+\lambda_{13}+\lambda_{\mathrm{Ps}})=0.34$. This places an upper limit of 34% on the trapping of positrons in the first stage. Trapping can be improved by injecting positrons with lower energy. However, due to the perpendicular component of the energy of the positrons as they are produced in the moderator, the total energy must be increased to allow the positrons to enter over the potential of electrode 0 [18].

TABLE I. Parameters used for the fits to the data shown in Fig. 3. The major uncertainty is the gas pressure in the first stage of the trap, which is not known better than a factor of 3. However, the relative importance of the various effects should not be affected. The corrected cross section is determined by assuming the factor of 2.7 error in the first-stage pressure postulated in Sec. V C.

Parameter	Value $(\mathrm{Torr\ cm})^{-1}$	σ (cm^2)	$\sigma_{\mathrm{corrected}}$ (cm^2)	Interpretation of parameter
λ_{Ps}	43.0	1.22×10^{-15}	4.52×10^{-16}	Ps formation at 20 eV
λ_{12}	18.0	5.09×10^{-16}	1.89×10^{-16}	Electronic excitation at 20 eV
λ_{13}	4.0	1.13×10^{-16}	4.19×10^{-17}	Ionization at 20 eV
λ_{23}	4.8	1.36×10^{-16}	5.04×10^{-17}	Electronic excitation at 11 eV
λ_{out2}	1.6			Loss rate at 11 eV
λ_{out3}	3.6			Loss rate at 2 eV

IV. SINGLE-STAGE TRAPPING

In order to determine which mechanisms are responsible for the most efficient loss of energy, the trap was operated in a single-stage mode. This was achieved by introducing the trapping gas directly into stage III and setting the voltages so that only one trapping region existed. This allowed the study of energy loss as a function of positron energy.

The positrons were produced at 42 eV and guided into the trapping region over a 40-V potential barrier produced by the potential on electrode 3. Thus we measure the cross section for processes which lead to 2-eV or greater energy loss. The nitrogen pressure in the trapping region was 1.0×10^{-5} Torr. The potential of the trapping region was varied in order to vary the positron kinetic energy in this region [Fig. 1(b)]. The potential also varied as a function of position, so the positron energy plotted is the maximum kinetic energy in the trapping region. Positrons were added for 1 s and the contents were then dumped onto an annihilation plate to determine the relative number of trapped positrons by the amount of annihilation radiation produced.

The results (Fig. 4) show an efficiency as function of energy which is similar to the measured cross section for electronic excitation of N_2 by electrons [19]. However, unlike the electron case, the trapping rate drops abruptly at 18.5 and 29 eV. The shape of this curve may be interpreted in light of the analysis in the preceding section. The process of electronic excitation of nitrogen has a threshold around 7 eV, but the presence of vibrational modes of the electronically excited state causes a large increase in the number of states available as one increases in energy above threshold. The process of positronium formation, with a threshold of 8.8 eV in nitrogen, starts to become significant around 11 eV. This competition between electronic excitation and positronium formation results in a maximum in the trapping efficiency. At 18.5 eV, positrons which are trapped by an electronic excitation (approximate energy loss, 9 eV) still have enough energy to form positronium and become lost. The trapped positrons with energies between 18.5 and 29 eV are those which experienced two electronic excitation collisions before having the chance to form positronium. The drop at 29 eV is due to positrons having enough energy to undergo two electronic excitation collisions (approximate energy loss, 18 eV) and then being lost to positronium formation. In order for a positron of greater than 29 eV to become trapped, it must undergo three electronic excitation collisions without forming positronium—an unlikely occurrence.

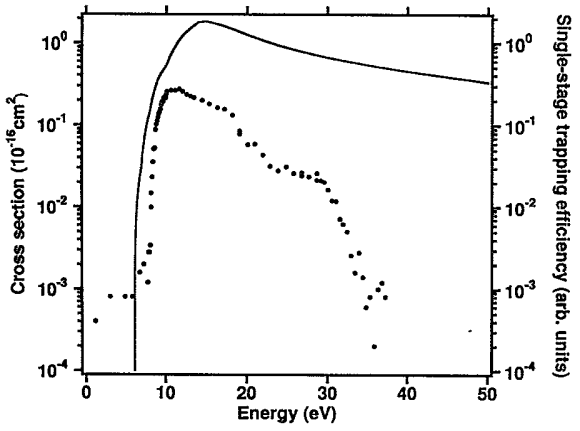

FIG. 4. Cross section for the electronic excitation of nitrogen by electrons (solid line) from Cartwright *et al.* [19], for comparison with the single-stage trapping efficiency (●). The data illustrate the threshold for trapping at 8 eV, and show that trapping processes involving positrons of less than 8 eV are almost three orders of magnitude less efficient than those in the energy range from 10 to 20 eV. The units for trapping efficiency are arbitrary.

The low number of positrons trapped at energies between 1 and 7 eV demonstrates that the processes leading to energy losses below 7 eV (e.g., vibrational and rotational excitation and momentum transfer) have small probability of causing sufficient energy loss to trap the positrons (in this case, 2 eV).

The energy range between the positronium formation threshold and the ionization energy of an atom or molecule is referred to as the Öre gap [20]. It is in this range of energies that the most efficient formation of positronium takes place in dense gases. In a similar manner, the most efficient trapping occurs between the energy of the first electronically excited state and the onset of positronium formation. Thus, we suggest the term "trapping gap" for this energy region.

V. MULTISTAGE TRAPPING

Single-stage traps do not provide efficient enough positron storage for our purposes, mainly because the high pressure required to trap positrons on a single pass results in a high annihilation rate and radial transport due to collisions. Instead, multistage methods are used to trap positrons on various time scales into regions with progressively lower electrostatic potential and background neutral density. In this section, we describe the dynamics of the positron distribution in the three-stage trap and its dependence on the nitrogen pressures and voltages of the stages.

A. Millisecond time scales

Early-time behavior of positrons shows a fast decay time which lasts for a few milliseconds to a few tens of milliseconds after the positrons are introduced into the trap. The character of this decay depends strongly on the voltage settings on the various stages of the trap. Figure 5 shows the results of a trapping experiment in which positrons were added to the trap for 5 ms, and then dumped onto an annihilation plate after a varying amount of store time, to determine the early-time behavior of the positrons. Three regimes exist, depending on the depth of the potential well of the third stage of the trap. The first regime is demonstrated by the curve corresponding to a 10-V potential well in stage III. In this case, the positrons have enough energy to form positronium in stage III. Thus, the trapping efficiency is small and

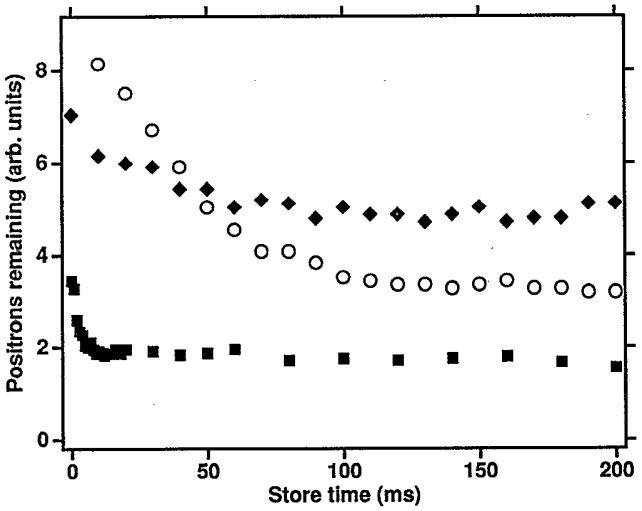

FIG. 5. Trapping of positrons at early times for different depths of the trapping region: (○) 4 V deep, (◆) 7 V deep, and (■) 10 V deep.

the early-time decay is quite fast, usually a few milliseconds. Only positrons which experience large energy losses before they can form positronium are trapped. We refer to this regime as the "deep-well" regime.

The second regime of interest is demonstrated by the curve corresponding to a 4-V potential well. The trapped-positron signal shows a decay which is much slower than the deep-well case, but the decrease in signal persists for a much longer time. This decay time shows no dependence on gas pressure, but is proportional to the magnetic field applied to the trap (Fig. 6). While a change in gas pressure does not affect the time scale of the decay, higher pressure does cause the decay to level off sooner. The observed loss of positrons is apparently due to magnetic or electric-field errors in the trap leading to transport of the positrons to the wall while they are still energetic enough to be in both the second and third stages. Thus, the higher pressure leads to quicker capture in the third stage and a faster leveling off of the decay. Realignment of the magnets has been shown to be effective in reducing this loss of positrons, but does not eliminate it completely (Fig. 7). The presence of this slow loss requires that the positrons become trapped quickly if efficient accumulation is to occur. We refer to this regime as the "shallow-well" regime.

The third regime of interest is the regime found to be optimum for trapping positrons and we refer to it as the "optimum configuration." In this regime, the potential difference between the second and third stages is approximately 7 V. If the positrons exist with several electron volts of kinetic energy in the second stage of the trap, then their kinetic energy lies within the trapping gap while in the third stage, and efficient trapping can occur.

B. Optimization of the trap voltages

Voltage scans of the last two stages of the trap were performed in order to find the combination of voltages which would lead to most efficient trapping (Fig. 8). Results show that the most efficient arrangement is such that approximately 7 V separates consecutive stages of the trap. At this voltage, positronium formation is not yet occurring, but a significant fraction of the positrons may undergo electronic excitation collisions with the nitrogen background gas.

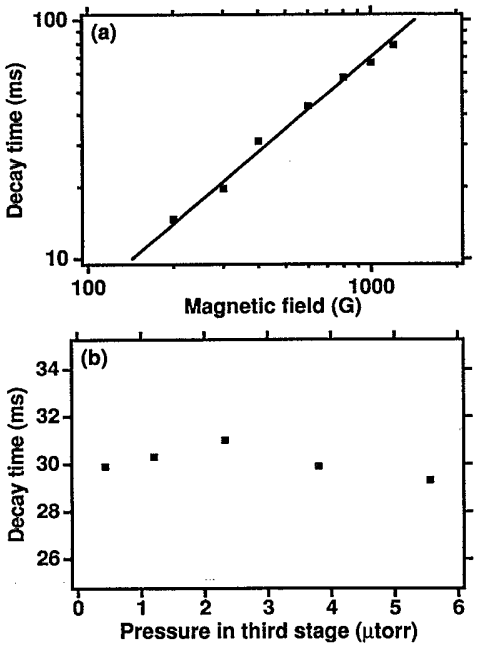

FIG. 6. Dependence of fast time decay in the "shallow-well" regime on (a) magnetic field and (b) nitrogen pressure. These data indicate a linear dependence on magnetic field and no dependence on pressure.

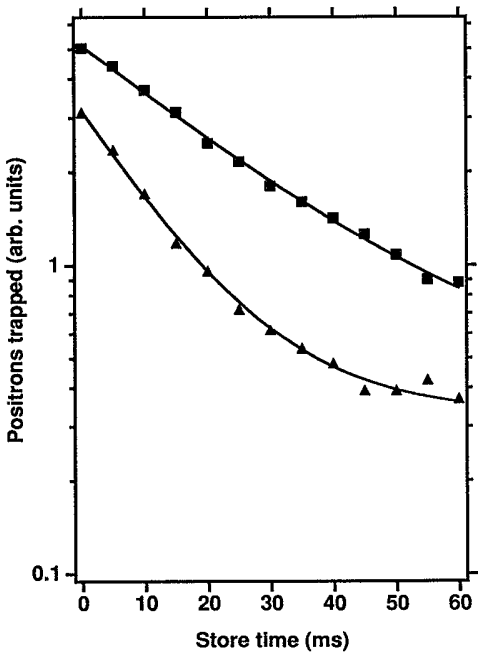

FIG. 7. Fast decay for a shallow well (▲) before and (■) after realignment of the magnets (see text for details).

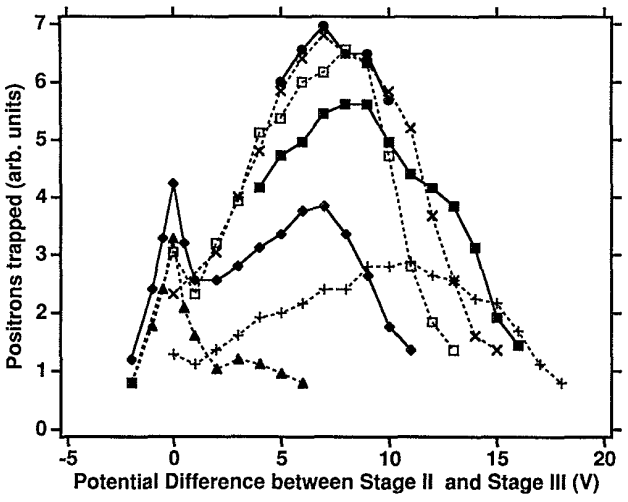

FIG. 8. Trapping efficiency vs the potential difference between the second and third stages with the potential of the third state at (+) 0, (■) 2, (×) 4, (●) 5, (□) 6, (♦) 8, and (▲) 12 V. The potential of the first stage was 18 V. Near the optimum trapping, there is a 7-V difference between the first and second stages and between the second and third stages.

C. Energy distributions

The parallel energy distribution of the positrons has been measured under a variety of conditions in order to follow the positrons as they lose energy in the trap. Measurements have been made as early as 50 μs after injection into the trap.

The measurements were made by slowly lowering the gate voltage on one end of the trap (Fig. 9). After a 100-μs pulse of positrons (approximately ten positrons) is injected into the trap, the gate voltage is lowered at a rate of 1 V/μs. When the potential on the axis has fallen below the parallel energy of a positron, that positron escapes from the trap and is deposited on the annihilation plate, creating detectable annihilation radiation. A start signal is sent to a time-to-amplitude converter at the beginning of the ramp-down of the gate. When a positron is detected, a stop signal is sent. The amplitude of the pulse coming from the time-to-amplitude converter is therefore a linear function of the parallel energy of the positron.

The voltage pulses on the moderator and the gate were provided by Wavetek Model 501 pulse generators with outputs amplified by 10. The pulse generator used to apply voltage pulses to the moderator was operated in a continuous mode, generating rectangular pulses of 100-μs duration. The pulse generator biasing the gate operated in triggered mode, deriving its trigger from the first pulse generator, and operating with a delayed output, the duration of the delay being varied to change the time of the energy distribution measurement. The duration of the injected pulse and the distance of the annihilation radiation detector were adjusted so that on average less than one

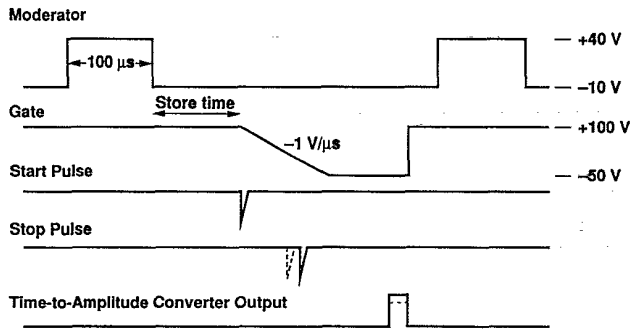

FIG. 9. Timing diagram showing the voltages on the moderator and gate electrodes and the timing of the start and stop pulses for the determination of time-dependent positron parallel energy distributions. The dashed signals correspond to a higher parallel energy positron which escapes earlier in the ramp-down of the gate voltage, leading to a lower amplitude pulse from the time-to-pulse-height converter.

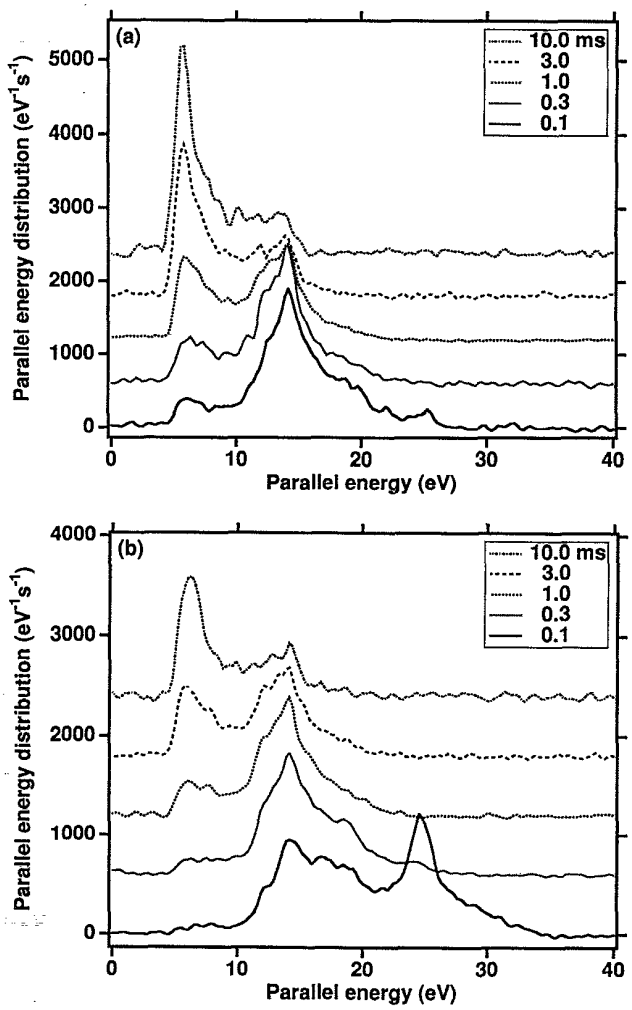

FIG. 10. Parallel energy distributions for store times of 0.1, 0.3, 1.0, 3.0, and 10.0 ms, for pressures in the trapping region of (a) 2.3 μTorr and (b) 0.58 μTorr. The vertical positions have been offset for clarity.

positron was detected per pulse, reducing the errors arising from detecting more than one positron per pulse.

Figures 10(a) and 10(b) show the results of two experiments for which the pressure was varied by a factor of 4 from one to the other. For Fig. 10(a), the pressure in the third stage of the trap was 2.3 μTorr, and in 10(b) the pressure was 0.58 μTorr. Parallel energy distributions are shown for times 0.1, 0.3, 1.0, 3.0, and 10.0 ms between injection of the positrons and the measurement of the parallel energy. Clearly shown are peaks corresponding to parallel energies necessary to travel through regions I, II, and III. For these experiments, the potentials of the stages were 25, 12, and 5 V. Electrode 2 (Fig. 1), which lies between stages I and II, was operated at 18 V, and provided a transition region between stages I and II.

The number of positrons in each stage can be followed as a function of time. Figure 11 shows the number of positrons in regions I, II, and III vs store time for the distributions in Fig. 10. Of interest are the ratios of the time constants for region I and region II. In the case of Figure 11(b), these time constants are $\tau_{\rm I}=78.8$ μs and $\tau_{\rm II}=5.08$ ms, indicating that the pressure in region II is 64 times that in region III. Pumping calculations lead to estimates of about 50, which is in good agreement with the measured value. Also, for Fig. 11(a), $\tau_{\rm II}=1.07$ ms, a factor of 4.75 lower than the value of $\tau_{\rm II}$ for the experiments in Figs. 10(a) and 10(b), in good agreement with the factor-of-4 change in the measured pressure. Using a positron energy of 10 eV, a pressure of 0.58 μTorr, and $\tau=5.08$ ms, we calculate a cross section of 5.1×10^{-17} cm^2 for the electronic excitation of nitrogen by positrons. This compares well with the value of 6.3×10^{-17} cm^2 for the electronic excitation of nitrogen by electrons [17]. It is a factor of 2.7 lower than that estimated by the single-pass data, but is within the errors of those measurements, given the uncertainty of the pressure in the first stage. The pressure measurements in the third stage are more accurate than in the first or second, having an uncertainty of approximately 10%. Therefore, this factor of 2.7 should probably be applied to the cross sections described above as measured in the first stage.

D. Cooling on nitrogen

The temperature of the positrons is measured using a magnetic analyzer [21,22]. The positrons are dumped onto a plate which can be biased to retard positrons of insufficient parallel energy. By changing the magnetic field at the annihilation plate, the perpendicular energy of the positrons is changed, due to conservation of $\mu\equiv\frac{1}{2}mv_\perp^2/B$ and therefore, so is the parallel energy. Thus, the change in parallel energy is directly related to the change in perpendicular energy, which we assume to have a Maxwellian distribution at temperature T_{e+}. Thus, by examining the curves of detected signal vs annihilation plate bias at two different magnetic-field strengths at the annihilation plate, a temperature may be determined [4].

The results, shown in Fig. 12, indicate that the positrons cool to room temperature with a rate which is proportional to nitrogen pressure, and equal to 0.55 ± 0.05 $s^{-1}\mu Torr^{-1}$. From Coleman [23], one would estimate

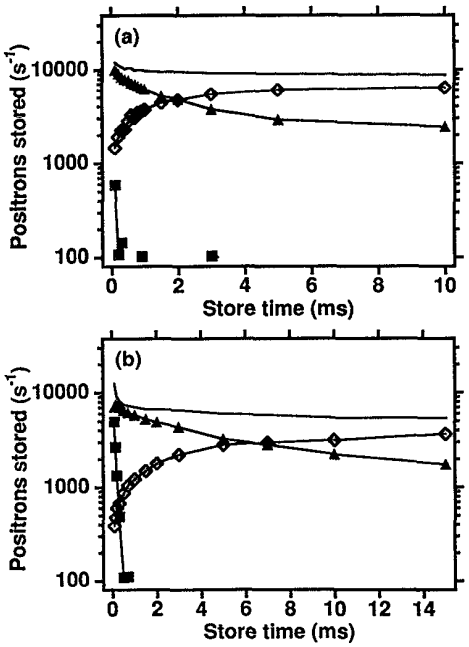

FIG. 11. Number of positrons with energy sufficient to travel in their bounce motion throughout (■) regions I, II, and III; (▲) regions II and III; and (◇) region III of the trap as a function of time for trapping-region pressures of (a) 2.3 μTorr and (b) 0.58 μTorr. The solid line represents the total of these three.

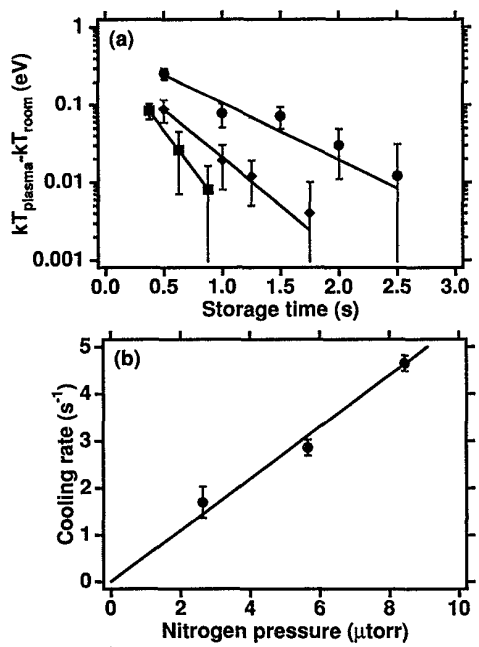

FIG. 12. (a) Positron temperature as a function of time at trapping region pressures of (●) 2.63 μTorr, (♦) 5.66 μTorr, and (■) 8.44 μTorr; and (b) the cooling rate vs pressure. These data indicate that the positrons cool in nitrogen with a rate of 0.55 ± 0.05 $s^{-1}\mu Torr^{-1}$.

approximately 0.34 $s^{-1}\mu Torr^{-1}$ for 100-meV positrons, if cooling is predominantly due to rotational-excitation and momentum-transfer collisions with nitrogen. Given the nature of Coleman's estimate, this can be considered good agreement.

E. Filling efficiencies

The filling efficiency is defined as the filling rate divided by the strength of the positron beam which passes completely through the trap in the absence of gas. Filling rate is defined as the rate of increase of trapped positrons for filling times much less than the annihilation time, but much longer than the trapping time. This filling rate was measured for several fill gas pressures, and the result is plotted in Fig. 13. Also plotted is the efficiency for positrons to lose enough energy that their kinetic energy is below the positronium formation threshold in the first stage on a single pass. The multistage results exceed the single-pass results at high pressure for two reasons. In the single-pass experiments at high pressures, when the analyzer potentials are more than about 10 V lower than that of the first stage, the positrons have a chance of forming positronium as they leave the first stage and travel to the annihilation plates. In the normal operation of the trap, this stage and subsequent stages are set to potentials which maximize the number of trapped positrons. In contrast, in the single-pass experiment, the analyzing electrode was scanned from 0 to 50 V, and the subsequent stages were at 0 V. In addition, in the normal operation of the trap, positrons which bounce off the gate potential have a second chance to become trapped as they return through stages II and I.

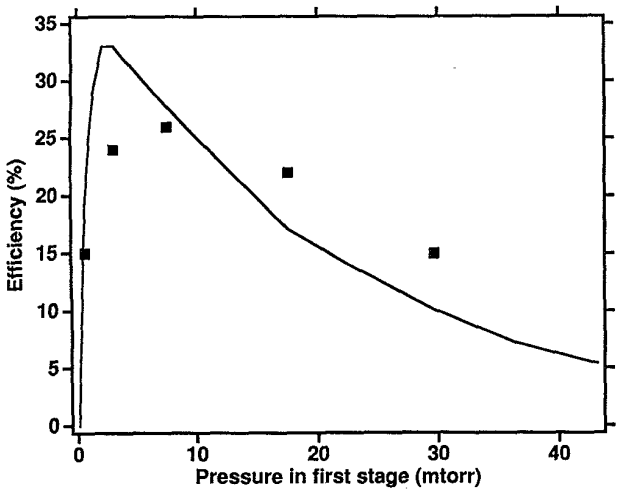

FIG. 13. Efficiency for positrons to lose enough energy to be below the positronium formation threshold on a single pass through the trap (solid line) and total trapping efficiency (■) as functions of pressure in the first stage

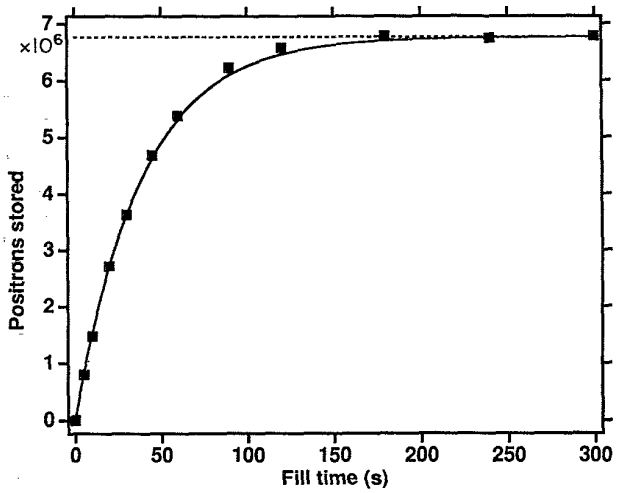

FIG. 14. Accumulation of positrons as a function of time. These data correspond to a filling rate of 1.73×10^5 s^{-1}, a lifetime of 39.1 s, and a maximum number of 6.8×10^6 stored positrons, using a 150-mCi ^{22}Na source.

F. Optimum trapping results

Figure 14 shows the accumulation of positrons as a function of time under optimum trapping conditions. For this run, a 150-mCi ^{22}Na source was used. The stored positron number was determined by measuring the charge collected on the annihilation plate after dumping the positrons. The solid line is a fit to the data of the form

$$N(t)=R\tau(1-e^{-t/\tau}) , \tag{3}$$

where $N(t)$ is the number of trapped positrons, τ is the lifetime of positrons in the trap, and R is the rate of trapping of positrons. A best fit occurs for $R=1.73\times10^5$ s^{-1}, $\tau=39.1$ s, and results in $N=6.8\times10^6$ stored positrons at times $t\gg\tau$ [18].

VI. CONCLUSIONS

Data indicate that electronic excitation is the predominant interaction of interest in the trapping of positrons in electrostatic wells. These collisions result in an energy loss of approximately 9 eV. Since the threshold for electronic excitation of nitrogen is close to the threshold for positronium formation, positronium formation puts a limit on the trapping rate possible with this method. At 11 eV, the processes of electronic excitation and positronium formation have about equal probabilities. Thus, a window exists for which efficient trapping can occur (i.e., the "trapping gap").

Current efforts have led to the accumulation and storage of approximately 1×10^7 positrons for a time limited by annihilation on the background nitrogen used for trapping and cooling the positrons. Cooling is accomplished by rotational and momentum transfer collisions with the background gas, and these reduce the temperature to within 10% of room temperature in about 2 s.

ACKNOWLEDGMENTS

The authors thank R. G. Greaves, E. A. Jerzewski, M. J. Penn, S. Tang, and M. D. Tinkle for their assistance in the operation of the positron trap and for taking some of the data presented in this paper. This work was supported by the Office of Naval Research.

*Present address: Lawrence Livermore National Laboratory, Livermore, CA 94551.

[1] P. B. Schwinberg, R. S. Van Dyck, Jr., and H. G. Dehmelt, Phys. Lett. **81A**, 119 (1981).

[2] C. M. Surko, A. Passner, M. Leventhal, and F. J. Wysocki, Phys. Rev. Lett. **61**, 1831 (1988).

[3] F. J. Wysocki, M. Leventhal, A. Passner, and C. M. Surko, Hyperfine Interact. **44**, 185 (1988).

[4] C. M. Surko, M. Leventhal, and A. Passner, Phys. Rev. Lett. **62**, 901 (1989).

[5] C. M. Surko, A. Passner, M. Leventhal, and F. J. Wysocki, in *Positron Annihilation,* edited by L. Dorikens-Vanpraet, M. Dorikens, and D. Segers (World Scientific, Singapore, 1989), pp. 161–170.

[6] V. Tsytovich and C. B. Wharton, Comm. Plasma Phys. Cont. Fusion **4**, 101 (1978).

[7] C. M. Surko, M. Leventhal, W. S. Crane, A. Passner, F. J. Wysocki, T. J. Murphy, J. Strachan, and W. S. Rowan, Rev. Sci. Instrum. **57**, 1862 (1986).

[8] C. M. Surko, M. Leventhal, W. S. Crane, and A. P. Mills, Jr., *Positron Studies of Solids, Surfaces and Atoms, A Symposium to Celebrate Stephan Berko's 60th Birthday,* edited by K. F. Canter, W. S. Crane, and A. P. Mills, Jr. (World Scientific, Singapore, 1986), pp. 221–233.

[9] T. J. Murphy, Plasma Phys. Cont. Fusion **29**, 549 (1987).

[10] A. Passner, C. M. Surko, M. Leventhal, and A. P. Mills, Jr., Phys. Rev. A **39**, 3706 (1989).

[11] M. Leventhal, A. Passner, and C. M. Surko, in *Annihilation in Gases and Galaxies,* edited by R. J. Drachman, NASA Conf. Publ. No. 3058 (NASA, Washington, D.C., 1989), pp. 273–283.

[12] T. J. Murphy and C. M. Surko, J. Phys. B **23**, L727 (1990).

[13] T. J. Murphy and C. M. Surko, Phys. Rev. Lett. **67**, 2954 (1991).

[14] B. L. Brown, W. S. Crane, and A. P. Mills, Jr., Appl. Phys. Lett. **48**, 739 (1986).

[15] N. E. Gramsch, J. Throwe, and K. G. Lynn, Appl. Phys. Lett. **51**, 1862 (1987).

[16] N. Zafar, J. Chevallier, G. Laricchia, and M. Charlton, J. Phys. D **22**, 868 (1989).

[17] J. H. Malmberg and C. F. Driscoll, Phys. Rev. Lett. **44**, 654 (1980).

[18] Subsequent to this work, this lower-injection-energy mode of operation was achieved with a moderator which produced moderated positrons of lower perpendicular energy. This permitted operating with a moderator-to-first-stage difference of about 9 V and resulted in trapping 1.5×10^7 positrons and a total trapping efficiency improvement of a factor of 2. These results will be published elsewhere.

[19] D. C. Cartwright, S. Trajmar, A. Chutjian, and W. Williams, Phys. Rev. A **16**, 1041 (1977).

[20] A. Ore, Naturvidenskap Rikke No. 9, University of Bergen, Årbok, 1949.

[21] D. Boyd, W. Carr, R. Jones, and M. Seidl, Phys. Lett. **45A**, 421 (1973).

[22] A. W. Hyatt, C. F. Driscoll, and J. H. Malmberg, Phys. Rev. Lett. **59**, 2975 (1987).

[23] P. G. Coleman, T. C. Griffith, and G. R. Heyland, J. Phys. B **14**, 2509 (1981).